

Rapid evaluation of gain spectra from measured ASE spectra of travelling-wave semiconductor optical amplifier

Qingyuan Miao (缪庆元), Dexiu Huang (黄德修), Deming Liu (刘德明),
Tao Wang (王涛), and Xiaofei Zeng (曾小飞)

Department of Optoelectronic Engineering, Huazhong University of Science & Technology, Wuhan 430074

Received August 13, 2004

An analytical equation, which directly relates amplified spontaneous emission (ASE) with small signal gain (SSG) of travelling-wave semiconductor optical amplifier (TWA), was derived. It was shown by theoretical analysis and experimental results that calibrated ASE spectra of TWA at different injection currents could be good evaluation and extension of SSG near gain peaks when gain peaks are larger than several decibels. The rapid evaluation method of SSG spectra is very simple, effective and especially applicable to batch measurement.

OCIS codes: 250.5980, 300.6170, 230.7020.

Small signal gain (SSG) spectra of travelling-wave semiconductor optical amplifier (TWA) are usually obtained from the ratio of amplified signal power to the input signal power for one by one wavelength at different injection currents. This conventional measuring method is not only tedious but also restricted by the wavelength range of external laser source. Amplified spontaneous emission (ASE) spectra are good sources of optical gain information. A method was introduced by Hakki-Paoli (HP)^[1], which detects the Fabry-Perot (FP) resonance depths superposed on ASE to deduce the optical gain. This method has been widely used to characterize semiconductor lasers^[2,3]. In TWA, owing to the significant reduction in facet reflectivity, especially the usage with a tilted waveguide, very small inexplicit ripple on ASE spectra invalidates the HP method.

In this paper, we derive an analytical equation, in which SSG spectra is directly related with the overall shapes of ASE spectra rather than the FP resonance depths superposed on ASE of TWA. Based on strictly theoretical analysis, calibrated ASE spectra of TWA are expected to be the approximate measurements of SSG spectra to a certain extent. In experiment, calibrated ASE spectra are carefully compared with the directly measured SSG values at different injection currents for the first time to our knowledge, which demonstrates and further clarifies the rapid evaluation method of SSG spectra.

A rigorous analysis of the relationship between SSG G_s and ASE intensity I_a is as follows.

To a TWA, facet reflectivity $R = 0$ is assumed. In this case, G_s is given by^[4]

$$G_s = \exp(g_{\text{net}}L), \quad (1)$$

$$g_{\text{net}} = g_m - \alpha_i = \Gamma g - \alpha_i, \quad (2)$$

where g_{net} is the net modal gain coefficient, g_m is the modal gain coefficient, g is the material gain coefficient, Γ is the optical confinement factor, α_i is the intrinsic loss coefficient, L is the length of TWA.

ASE intensity I_a is connected with g_{net} by^[5,6]

$$I_a = \frac{SI_s}{g_{\text{net}}} [\exp(g_{\text{net}}L) - 1], \quad (3)$$

where S is the cross-sectional area of the excited volume, I_s is the spontaneous emission intensity per unit volume.

Owing to the fundamental relationship between stimulated and spontaneous emission rates, the modal gain coefficient $g_m = \Gamma g$ can be determined from the spontaneous emission using^[7,8]

$$g_m = C_p \frac{I_s}{E^3} \left[1 - \exp\left(\frac{E - \Delta E_f}{kT}\right) \right], \quad (4)$$

where energy $E = hc/\lambda$, h is Planck constant, c is the speed of light in free space, and λ is the corresponding wavelength; C_p is a fitting constant which accounts for the fact that only relative values for I_s are determined experimentally; k is the Boltzmann constant; T is the temperature; ΔE_f is the quasi-Fermi level separation.

By combining Eqs. (1)–(4) and eliminating I_s , the following equation, which directly relates I_a with G_s , is obtained:

$$\begin{aligned} & \frac{\lambda^3 I_a}{h^3 c^3} \left[1 - \exp\left(\frac{hc - \lambda \Delta E_f}{\lambda kT}\right) \right] \\ &= C_k \left(1 + \frac{\alpha_i L}{\ln(G_s)} \right) [G_s - 1], \end{aligned} \quad (5)$$

where $C_k = S/C_p$.

Equation (5) is the theoretical basis of the rapid evaluation method of the SSG spectra for TWA. It reveals that I_a is approximately proportional to G_s when G_s is large enough ($G_s \gg 1$ dB). That is to say, the shapes of ASE spectra are similar to those of SSG spectra when G_s is large enough. Because gains decrease gradually departing from gain peaks, further deduction is that calibrated ASE spectra can be directly used to evaluate the SSG spectra near gain peaks when gain peaks are larger than several decibels. The larger the SSG values are, the more accurate the evaluation results will be.

In experiment, the device under test is an Opto Speed 1550CRI TWA, which is a bulk InGaAsP/InP structure grown by metal organic chemical vapor deposition (MOCVD). The device has low polarization dependence and low ripple. The 3-dB saturation output power is 6 dBm. Low ripple is obtained by tilting the amplifier optical waveguide by 12° in respect to the amplifier facets and by application of double layer dielectric anti-reflection coatings. The thermal effects which would result in a red shift of the bandgap energy have been removed by using a Peltier element and a 10-kΩ thermistor for device temperature stabilized at 20 °C. In order to obtain a wide spectrum continuous wave (CW) signal source, an EXFO FLS-2600B tunable laser source is used together with a Velocity tunable diode laser. The input optical signal power is set at -25 dBm, which means that the signal gains are measured under the unsaturated condition. The directly measured SSG values at different injection currents are shown in Fig. 1. The ASE spectra taken from one facet of the TWA are recorded by an Agilent 86140B optical spectrum analyzer (OSA).

The detected ASE spectra at different injection currents are calibrated using the SSG value at ASE peak wavelength at injection current 250 mA, which means making the ASE peak value at 250 mA equal to the given SSG value, as shown in Fig. 1. The carrier density in the active region increases with the increase of injection current. This yields band-filling effect, which enlarges the quasi-Fermi level separation ΔE_f between conduction band and valence band. As a result, the peaks of both the SSG spectrum and the ASE spectrum clearly shift toward shorter wavelengths, as shown by the arrows in Fig. 1. In the SSG measurement, the carrier density decreases because of the carrier consumption arising from the amplifying of input signal. It slightly reduces ΔE_f , which is inevitable during an actual SSG measurement. This makes the peak of the SSG spectrum have a slight red shift relative to the peak of the ASE spectrum. Although the peak wavelength of the ASE spectrum is not the same as that of the SSG spectrum, the SSG value at the ASE peak wavelength can be used as the SSG peak in the evaluation method because of the small difference between them. The comparison results between the calibrated ASE spectra and the directly measured SSG values at different injection currents are listed in Table 1, which tells us the wavelength ranges within which the deviation between the calibrated ASE spectra and the directly measured SSG values is no more than 1 dB. The corresponding measured SSG maxima are also listed. Experiment results indicate that the SSG spectra and the calibrated ASE spectra are similar near gain peaks when gain peaks are larger than several decibels. The larger the injection current is, the larger the SSG values are. As a result, a more wider wavelength range will be obtained, in which the shape of the calibrated ASE spectrum is similar to that of the SSG spectrum. This coincides with the forecast of Eq. (5). When injection current is 250 mA, the spectrum width reaches 80 nm with deviation ≤ 1 dB. So single-value calibrated ASE spectra are very good approximation and extension of SSG near gain peaks when gain peaks are larger than several decibels. Since ASE spectra can be easily obtained and only one SSG value is needed for

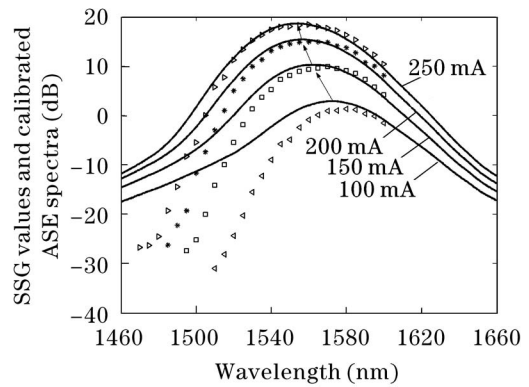


Fig. 1. The directly measured SSG values (symbols) and the calibrated ASE spectra (solid curves) at different injection currents. The arrows indicate the peak shifts of both the SSG spectrum and ASE spectrum.

Table 1. Comparison Results

Injection Current (mA)	SSG Maximum (dB)	Wavelength Range with Deviation ≤ 1 dB (nm)
250	18.4	1520—1600
200	14.9	1540—1590
150	9.9	1555—1600
100	1.3	1585—1600

calibration, the evaluation method can rapidly provide some valuable information such as the full width at half maximum (FWHM) of the SSG spectra at different injection currents. The rapid evaluation method of SSG spectra is very simple and easy to use.

Far from gain peaks, SSG values are too small to satisfy the condition of the evaluation method predicted by Eq. (5). There are increasing deviations between the calibrated ASE spectra and the directly measured SSG values along with the increasing apartness from gain peaks, as shown in Fig. 1. The smaller the injection current is, the smaller the SSG values are, then there are more deviations between the calibrated ASE spectrum and the directly measured SSG values. Therefore the evaluation condition should be noticed when using the method.

In conclusion, it was shown by theoretical analysis and experiment results that single-value calibrated ASE spectra of TWA at different injection currents are good evaluation and extension of SSG around gain peaks when gain peaks are larger than several decibels. The rapid evaluation method of SSG spectra is very convenient, effective, and especially applicable to batch measurement.

In addition, based on Eq. (5), extended SSG spectra with a wavelength range as wide as ASE spectra can be derived from measured ASE spectra at different injection currents. The extension method, which can overcome the limitation of wavelength range, will be reported elsewhere.

This work was supported by the National “973” Project of China (No. G2000036605), the National “863” Program of China (No. 2002AA312160), and the Science and Technology Foundation of Wuhan City. Q. Miao’s e-mail address is mqy_hust@yahoo.com.cn.

References

1. B. W. Hakki and T. L. Paoli, *J. Appl. Phys.* **44**, 4113 (1973).
2. W.-H. Guo, Q.-Y. Lu, Y.-Z. Huang, C.-L. Han, and L.-J. Yu, *Acta Opt. Sin.* **23**, (suppl.) 331 (2003).
3. M. Lerttamrab, S. L. Chuang, C. Gmachl, D. L. Sivco, F. Capasso, and A. Y. Cho, *J. Appl. Phys.* **94**, 5426 (2003).
4. M. J. O'Mahony, *J. Lightwave Technol.* **6**, 531 (1988).
5. K. L. Shaklee, R. E. Nahori, and R. F. Leheny, *J. Lumin.* **7**, 284 (1973).
6. S. L. Chuang, *Physics of Optoelectronic Devices* (John Wiley and Sons, New York, 1995) p.407.
7. C. H. Henry, R. A. Logan, and F. R. Merritt, *J. Appl. Phys.* **51**, 3042 (1980).
8. M. P. Kesler and C. Harder, *IEEE J. Quantum Electron.* **27**, 1812 (1991).